R. & M. No. 3502

MINISTRY OF TECHNOLOGY

AERONAUTICAL RESEARCH COUNCIL
REPORTS AND MEMORANDA

The Flow Produced by Interaction of a Turbulent Boundary Layer with a Normal Shock Wave of Strength Sufficient to Cause Separation.

By J. Seddon, Ph.D.

LONDON: HER MAJESTY'S STATIONERY OFFICE
1967
PRICE 15*s.* 6*d.* NET

The Flow Produced by Interaction of a Turbulent Boundary Layer with a Normal Shock Wave of Strength Sufficient to Cause Separation.

By J. Seddon, Ph.D.

Reports and Memoranda No. 3502*

March, 1960

Summary.

The nature of normal-shock and turbulent-boundary-layer interaction is described on the basis of an experiment involving two-dimensional flow, at $M = 1{\cdot}47$, over a flat plate. Special attention is paid to the flow development downstream of separation. Conditions governing reattachment are observed and the nature of the eddy-flow bubble is shown.

Compatibility requirements between the viscous and non-viscous flows are described. In the viscous layer itself the flow is shown to undergo successively the three processes of shock compression, displacement and rehabilitation.

For an interaction in which no mainstream constraints are applied, separation occurs at a point two boundary-layer thicknesses downstream of the start of interaction, and reattachment at 12 thicknesses. Rehabilitation, however, is still incomplete at 50 thicknesses.

Velocity profiles are examined in relation to the Coles wake hypothesis. Over the greater part of the flow this hypothesis is found to hold true. It does not hold in the immediate vicinity of the shock wave or in other regions of strong pressure gradient. An empirical extension is suggested to take account of the variations observed.

LIST OF CONTENTS

*Replaces R.A.E. Tech. Memo. No. Aero. 667 — A.R.C.22 637.

LIST OF CONTENTS—*continued*

LIST OF ILLUSTRATIONS

Figure

---

1. *Introduction.*

The interaction between a turbulent boundary layer and a normal shock wave is a feature frequently encountered in modern aerodynamics. It occurs, for example, in the flow round aerofoils at transonic speeds (Fig. 1a), as has been described by Pearcey[1]. Other important instances are to be found in the aerodynamics of supersonic intakes. In the case of a normal-shock inlet with external (i.e. extraneous) boundary layer (Fig. 1b), the shock wave and boundary layer interaction occurring ahead of or in the plane of the inlet can be responsible for a large loss in intake delivery pressure. This situation has been described by Seddon and Haverty[2] and subsequently analysed more fully by Seddon[3]. A similar situation exists in the case of external-compression inlets with terminal normal shock (Fig. 1c): here, in addition to the loss of total pressure involved, the interaction is closely linked – as has been discussed by Griggs and Goldsmith[4] and others – with the onset of flow instability known as intake buzz. A fourth example concerns the flow in a closed diffuser (Fig. 1d), as in a supersonic wind tunnel or in a supersonic intake when operating supercritically. In this case an effect which is liable to be more important than the drop in total pressure is a loss of uniformity in flow velocity and direction.

Much valuable work on the fundamental nature of shock and boundary layer interaction has been done by Gadd[5], Bogdonoff[6], and others. In the context of the class of problems just described, however, it seemed on inspection that there were two aspects of the general phenomenon which particularly called for further study. In the first place, most of the experimental work had been concerned with the interaction produced by oblique shocks: some clarification of the general character of a normal-shock interaction was required. Secondly, while much attention had been paid to features such as the pressure rise to separation and the extent of upstream influence of the shock wave, there was little evidence relating to the development of flow downstream of an interaction and in particular to the conditions governing flow reattachment.

When, therefore, the opportunity to carry out a fundamental study was presented, by virtue of the author's temporary allocation to GALCIT* during the tenure of a Commonwealth Fund Fellowship

---

*Guggenheim Aeronautical Laboratory, California Institute of Technology, Pasadena, California, U.S.A.

(1955–56), it was decided to study the shock and boundary-layer interaction problem from the particular aspects described above. An experiment was devised in the following terms:

(1) The interaction was to be between a turbulent boundary layer and a normal shock.

(2) The shock strength was to be sufficient to cause separation. (This, it was known[2], required an upstream Mach number in excess of about 1.3.)

(3) Flow development downstream of the interaction would be examined and, if possible, controlled by means of flow constraints applied outside the region of interaction itself.

This experiment forms the basis of the present paper. A description is given and from the results the fundamental nature of normal shock and turbulent layer interaction is discussed in general terms.

A particular feature concerns the detailed examination of velocity profiles throughout the extent of flow affected by the interaction. Interesting evidence is obtained both in support of and also qualifying the hypothesis of Donald Coles[7] concerning profile similarities in the development of the turbulent layer under arbitrary pressure gradients.

2. *Description of Experiment.*

2.1. *Experimental arrangement.*

The tests were made in the 10 in. × 4 in. 'Transonic Tunnel' of the Guggenheim Aeronautical Laboratory. The tunnel was operated purely as a supersonic tunnel, and run at its top Mach number (1·47) throughout.

The experimental arrangement is illustrated in Fig. 2. The boundary layer was generated on a horizontal flat plate spanning the 4 in. dimension of the tunnel and mounted 4 in. above the floor of the working section. The plate was insulated from the tunnel walls by means of thin rubber strips along its edges. With this arrangement, and in view of the modest Mach numbers involved, it was considered that heat transfer effects could be ignored.

Free stream Reynolds number was $4{\cdot}0 \times 10^6$ per foot, the appropriate actual value being $3{\cdot}0 \times 10^6$ at the principal measuring station, 9 in. from the plate leading edge. Total temperature was approximately 50 deg C.

To generate and locate the shock wave a second, shorter, plate was mounted above the first. The second plate ('shock generator') also spanned the tunnel: it was carried from a framework of struts which passed up through a slit in the roof of the tunnel to a traversing mechanism, by means of which the shock generator could be moved both horizontally and vertically relative to the boundary layer plate.

A full-span flap, angled downwards at a small angle, was provided at the rear of the generator plate: this formed a throttle at the end of the channel between the two plates. Over a range of vertical settings of the generator, the flow in this channel was essentially subsonic and a normal shock was produced in the mainstream ahead of the generator leading edge. By correctly positioning the generator, the shock could be located in any desired position; in particular it could be placed across the entry of the channel, i.e. just touching the leading edge of the generator plate.

Total-pressure surveys were made by traversing a single pitot-tube along a line normal to the surface of the boundary-layer plate, at a station on the plate centreline nine inches from the leading edge. Profiles corresponding to different streamwise stations of the interaction were obtained by moving the shock generator upstream or downstream, this carrying the shock wave with it. Fine vertical adjustments of the generator were employed to maintain the shock in a desired position relative to the generator leading edge.

Plate static pressures were measured over a short distance along the centreline, including the nine-inch position. Overlapping fragments of pressure distribution were thus obtained for different positions of the shock generator.

Static pressures normal to the plate were occasionally recorded by substituting a static tube for the normal pitot tube in the traversing arrangement.

Apparatus was available for continuous-schlieren viewing of the flow and also for spark-schlieren photography.

Concerning the question of possible three-dimensional effects, no detailed investigation of the tunnel sidewall boundary layers was made, but it was considered that adequate evidence of two-dimensionality of flow on the tunnel centreline was provided by the results of preliminary surface flow visualisation on the plate, the use of one or two offset static pressure points and the general appearance of schlieren pictures.

2.2. *Undisturbed Boundary Layer.*

The boundary layer was made turbulent by roughening the surface of the plate along a narrow strip close to the leading edge. In the early part of the work some evidence of deterioration of the roughness effect was observed – caused presumably by dust contamination and wear. To supplement the effect, therefore, a line of small bleed holes was drilled through the plate immediately downstream of the roughness (Fig. 2). These provided air jets blowing through automatically from the chamfered undersurface (i.e. pressure side) of the plate.

The combination of roughness and air jets resulted in a boundary layer of reasonable thickness, suitable profile and repeatable characteristics. The thickness at the measuring station was 0·16 in.* The velocity profile is given in Fig. 3, where also the relative size of the pitot tube is shown.

Since the method of making a streamwise survey of shock and boundary layer interaction involved moving the shock along the plate, it was necessary to correct continuously for a variation of initial boundary-layer thickness** with shock position. As a check on the variation of thickness with distance along the plate, schlieren observations were made of the height (above the plate surface) of the point of shock bifurcation which is a constant feature of the interaction. For a given form of interaction this height is proportional to the initial boundary-layer thickness. The height is plotted in Fig. 4, where it is seen that a 4/5 power law in distance fits convincingly. It was therefore assumed that over the range required, a similar law existed for the variation of initial boundary-layer thickness.

2.3. *'Basic' and 'Modified' Interactions.*

The flow development downstream of the shock wave was constrained by the presence of the shock generator. Originally it had been intended that the form of this constraint should be varied as widely as possible, by changing, for example, the height of the generator above the plate, the angle of the throttle flap, or the inclination of the whole generator.

It was found, however, that any reasonably complete survey of the streamwise flow development involved large fore-and-aft movements of the generator plate and shock wave. The resulting variations of initial boundary-layer thickness led to difficulties in resetting the generator so as to reproduce identical conditions downstream, difficulties which in most cases could not readily be overcome. Moreover, in no case could asymptotic downstream conditions be reached before the flow passed through the pressure field of the angled throttle flap.

One case, however, could be reproduced with reasonable exactness throughout the survey, namely that in which the generator plate was horizontal (i.e. parallel to the boundary-layer plate) and the shock wave was located at the leading edge of the generator (Fig. 5b). This case was investigated fully and is termed the 'modified' interaction.

Furthermore, it was found that by locating the generator well downstream and using a fairly large angle of the throttle flap, a normal shock could be positioned across the complete upper channel, i.e. between the boundary-layer plate and the tunnel roof (Fig. 5a); and its fore-and-aft position could be controlled accurately by traversing the generator in the usual way. Under these conditions it was adjudged that the degree of constraint upon the development of flow from the interaction at the plate surface was small. In effect, a constraint-free interaction had been obtained, subject only to the conditions at infinity

---

*Thickness defined to the point where $u/u_1 = 0{\cdot}999$.

**Initial boundary-layer thickness means the thickness of the undisturbed layer at the start of an interaction.

being those upstream and downstream of a plane normal shock. This case was also investigated fully and is termed the 'basic' interaction. It was found that asymptotic downstream conditions were, in fact, closely approached without interference from the throttle flap.

The main discussion of the paper centres upon results for the two interactions described above and shown schematically in Fig. 5. Essential characteristics of the flow are discussed in terms of the basic interaction. Some effects of arbitrary constraints, which in practice determine the differences in flow that arise in various applications, such as those mentioned in the introductory section, can be deduced qualitatively. Results for the modified interaction are used for the purpose of analysing the detail development of velocity profiles under a particular set of pressure gradients.

3. *General Character of Basic Interaction.*

3.1. *Schlieren Observation.*

A schlieren photograph (Fig. 6) reveals some important features of the basic interaction. At a height above the plate equal to between 5 and 6 times the thickness of the undisturbed layer the normal shock bifurcates. The front leg of the bifurcated system inclines down into the boundary layer at about 53 deg angle. Flow separation occurs at the foot, the edge of the viscous layer being turned away from the plate through approximately $7\frac{1}{2}$ deg. These values of shock angle and angle of turn are mutually consistent for the flow outside the viscous layer at the particular value of free stream Mach number.

The second shock of the bifurcated system is S-shaped. It leaves the bifurcation point in a direction normal to the flow behind the front leg; lower down it inclines backwards from this normal; on entering the viscous layer it appears to revert to a normal direction. This suggests that behind the second shock the flow is mixed, being subsonic near the bifurcation, supersonic lower down and of course subsonic again within the viscous layer. Pressure traverses (Section 3.2) confirm that this is actually the case.

It is clear that the thickness of the viscous layer is greatly increased by the interaction. No. indication is given as to whether the flow reattaches to the surface after the initial separation.

A further marked feature is the trace of a vortex sheet springing from the bifurcation point. This is present because the flows above and below the sheet, at a given streamwise station, have equal static pressures but different total pressures (owing to the different shock systems) and hence are at different Mach numbers.

3.2. *Static-pressure Distributions.*

Static pressures recorded on the surface of the plate are plotted in Fig. 7. From the different positions of the shock wave, controlled by the shock generator, a series of fragmentary pressure distributions is obtained, each fragment being indicated by a separate symbol in the diagram. It is seen that by plotting streamwise position in terms of the undisturbed boundary-layer thickness corresponding to a particular position of the shock, a single consistent curve is obtained for the overall pressure variation. This is compared in the diagram with the distribution for normal shock flow, obtaining at a sufficient distance from the surface.

An initial sharp pressure rise to the separation point is observed. The pressure ratio at separation (kink pressure to upstream pressure) is 1·48 which, for the free stream Mach number 1·47, agrees reasonably with the observations of Gadd and others. The distance of the separation point from the start of interaction is about 2 boundary-layer thicknesses.

After separation, the pressure gradient is much reduced but the pressure nevertheless continues to rise steadily, tending asymptotically towards the downstream value for a normal shock. At a distance downstream equal to 60 boundary-layer thicknesses, however, the pressure rise achieved is still only 90 per cent of that in the normal shock.

A singnificant result is that the pressure variation after separation is smooth. Apparently reattachment, if it occurs, does not control the pressure development in the way that separation does.

It is of interest to note in passing that the total upstream spread of the interaction, as measured from the position of the normal shock, is about five times the undisturbed boundary-layer thickness.

Assuming that transverse pressure gradients through the viscous layer are small (*see* below) the Mach number at the edge of the layer may be calculated from the pressure on the plate and the total pressure behind the observed shock system. [For this purpose the total pressure is not significantly different from the initial free-stream value.] Mach number so calculated is plotted in the lower part of Fig. 7. The results show that supersonic flow persists well downstream of the shocks and suggest that a smooth deceleration through to subsonic speeds is obtained.

This situation is further revealed by the results of static-pressure traverses made normal to the surface of the plate at a few streamwise stations using a static tube in place of the traversing pitot. Examples of these are shown in Fig. 8. Characteristics of the results are:

(1) the pressure is approximately constant across the viscous layer;

(2) in passing from the edge of the viscous layer to the vortex sheet, the pressure increases steadily;

(3) above the vortex sheet the pressure is again approximately constant.

Corresponding Mach-number variations outside the viscous layer are shown in the lower part of the diagram. Where the Mach number at the edge of the layer is supersonic, a smooth variation through to subsonic values is found on traversing out towards the vortex sheet. Thus a 'tongue' of supersonic flow is defined, extending downstream of the shock system for a distance of, in this case, some 13 times the initial boundary-layer thickness from the start of interaction.

3.3. *Total Pressure Traverses.*

Mach number profiles through the viscous layer, obtained from total-pressure traverses at several streamwise stations, are given in Figs. 9 and 10. Fig. 11 shows the corresponding non-dimensional velocity profiles.

The occurrence of flow separation shortly downstream of the start of interaction is confirmed. Profile (2) – Fig. 9 – is a near-separation profile.

A closed bubble, with circulating eddy flow, exists downstream of separation. Reversed-flow velocities in the lower part of the bubble were measured in one case – profile (5) – by reversing the direction of the pitot tube, re-positioning the shock and using a special water manometer to record the low dynamic pressures. Maximum reversed velocities are seen to be of order 0·1 in Mach number.

The shape and size of the bubble, as determined from the profiles, are shown in detail in Fig. 12. The maximum height is, for the case investigated, quite small – about half the initial boundary-layer thickness. This was to be expected, since the free stream Mach number (1.47) was not greatly in excess of the minimum value necessary to cause separation of a turbulent layer, and no further pressure gradients were imposed on the flow. The unsymmetrical shape is interesting – in the growing stage the surface of the bubble is first concave, then convex, and maximum height is attained at about 70 per cent of bubble chord. It will be seen later in the Report how these features conform to a natural development of the complete profile within the viscous layer.

Reattachment, or bubble closure, occurs at a position some 12 times the initial boundary-layer thickness downstream of the start of interaction. At this position the pressure on the surface is rising smoothly towards its asymptotic value, and the occurrence of reattachment, contrary to that of separation, does not produce any singular effect (Fig. 12). Reattachment, it seems, is in the nature of an incidental occurrence in an extended process of turbulent mixing following separation, and it is the overall mixing process which rehabilitates the boundary layer. The mixing becomes the dominant feature shortly after the separation – the inflexion point in the bubble contour is probably evidence of this – and, as the Mach profiles show, has not been completed at a downstream distance of 50 initial thicknesses.

Further characteristics of the viscous layer, deducted from the profiles, are plotted in Figs. 13 to 15. Thickness and displacement thickness (Fig. 13) are approximately constant up to separation (compare also profiles (1) and (2), Fig. 9) but both increase rapidly in the phase immediately following. This corresponds to the outer flow having been turned away from the wall on passing through the leading shock. At reattachment the thickness is close on double that of the undisturbed layer. Downstream of reattachment, during the rehabilitation process of the profiles, the growth of thickness is again rapid, the rate being about three times that of the undisturbed layer. This corresponds to a phase of rapid entrainment of flow into the viscous layer, as is shown by the plot of mass flow, Fig. 14.

An interesting feature in the variation of form parameter, δ^*/θ (Fig. 13), is that widely-differing values are obtained at the points of separation and reattachment. Anticipating the further discussion of profile characteristics which follows in Section 5, we note that the value of δ^*/θ at reattachment (about 4.3) is in agreement with that suggested by Coles[7], but the value at separation is much lower.

The plot of streamlines in Fig. 15 indicates an outward curvature, near the wall, behind the leading shock. This is consistent with the continued pressure rise along the wall shown in Fig. 7 and also with the shape of the bubble as already observed.

Changes of stream-tube area corresponding to either supersonic or subsonic compression in the region of mixed flow outside the viscous layer are barely detectable, owing to the fact that Mach numbers in this region are not greatly different from unity. The shape of the vortex sheet, however, is interesting and indicates how this sheet, carrying, as has been seen, a transverse discontinuity in velocity but no discontinuity in pressure, forms a controlling link between the interaction flow and that through the unchanged normal shock. If the position of the vortex sheet is altered by application of a different set of boundary conditions in the outer stream, then continuity requirements in the flow between the sheet and the surface must lead to modification of any or all of the characteristic features of the interaction.

In passing, it is interesting to note the degree of persistence of the vortex sheet in the downstream flow, despite (in the present case) a relatively small velocity discontinuity as was shown in Fig. 8. A second schlieren photograph of the interaction (Fig. 16) shows the sheet to persist quite clearly up to 35 boundary-layer thicknesses: in actual fact it was observed plainly over the total range of investigation.

3.4. *Summarising Discussion.*

The principal features of the flow created by constraint-free interaction of a turbulent boundary layer with a normal shock wave, of strength sufficient to cause separation, have been brought out at various points in the foregoing analysis. We can now construct a scaled representation of the physical flow as shown in Fig. 17.

The solution of a problem in viscous flow requires that different sets of conditions within the viscous layer and outside it be satisfied simultaneously. In the present situation it has been seen that the shock pressure rise causes separation and that the shock itself must bifurcate in order to match conditions in the flow immediately outside the viscous layer to the need for the viscous layer itself, having separated, to flow (temporarily at least) away from the surface. It follows that the total flow is in this case divided into three régimes:

(1) the outer, or mainstream, flow passing through the normal shock;

(2) an intermediate layer, in which the flow passes through the bifurcated shock system and is at different total pressure from the outer flow;

(3) the viscous layer;

and a solution to the flow depends upon conditions appropriate to each of the régimes being satisfied simultaneously.

In the basic interaction, the mainstream is effectively of infinite extent and the continuity condition of a bounded flow does not apply. There is, as the photographs show, some curving of the main shock as it approaches the bifurcation point and this leads to a grading of velocity towards the higher values of the intermediate layer. The main point, however, is that the vortex sheet, which forms the boundary between mainstream and intermediate layer, can take up a position as required by continuity conditions within the intermediate layer, without constraint from the outer flow.

Flow in the intermediate layer turns away from the surface on passing through the leading shock and back towards the surface (to a smaller extent) at the rear shock. A mixed flow exists behind the rear shock, supersonic near the viscous layer and subsonic near the vortex sheet. The supersonic tongue extends downstream for several units of distance and the edge of the viscous layer is the last part of the flow to go subsonic. This supersonic compression is apparently achieved without further shock waves.

In the viscous layer the overall process is conveniently broken down (streamwise) into three phases:

(1) the shock phase;

(2) the displacement phase;

(3) the rehabilitation phase.

The shock phase extends from the start of interaction to the separation point. It is characterised by a steep rise in pressure on the surface and a change in profile shown by comparing profiles (1) and (2) of Fig. 9. The thickness and displacement thickness of the layer are virtually unchanged.

In the displacement phase, the layer flows away from the surface and, corresponding to the development of a bubble, both total layer thickness and total displacement thickness are rapidly increased (Fig. 13). The steep pressure rise is checked at separation but a slow rise continues through the displacement phase, the streamlines outside the bubble being concave outwards from the surface.

The rehabilitation phase may conveniently be said to commence when the intermediate flow passes through the rear shock. In the viscous layer the approximately corresponding point is the inflexion point of the bubble contour (between profiles (5) and (6) in Fig. 9). Although the bubble continues to grow for for some distance, reversed-flow velocities are now on the decrease, as a prelude to the 'filling out' of the complete profile. In this early stage the rehabilitation takes place, largely by means of readjustment of shear gradients within the viscous layer itself. This explains why the pressure on the surface continues to rise although the streamlines are now concave inwards.

Beyond reattachment, entrainment of flow from the intermediate layer becomes increasingly active (Fig. 14) and is a primary mechanism of the rehabilitation process. Streamlines are once more concave outwards and remain so until rehabilitation is completed. These features, indeed, give some degree of significance to the reattachment point which, as was seen, is not revealed by the surface pressure distribution.

In the rehabilitation phase the flow is closely analogous to that downstream of a rearward-facing step or to that in a duct following a sudden increase in area. It is seen that reattachment will always occur, provided of course that the solid surface extends sufficiently far downstream.

4. *Constrained Interactions.*

4.1. *Some Thoughts and Examples.*

The course of an interaction may be modified in, broadly speaking, either of two ways. One, the indirect way, is by the introduction of constraints into the mainstream flow. This imposes a set of conditions, to satisfy which the vortex sheet position requires to be different, in general, from that appropriate to the basic interaction. Equilibrium between conditions in the intermediate and viscous layers is thereby disturbed and the consequent readjustment affects the viscous-layer characteristics – size of bubble, location of reattachment and overall growth of the viscous region. Such changes are of especial significance in connection with intake and duct flows (Figs. 1b to d), where mainstream constraints take the form of particular duct area distributions, prescribed amounts of spillage, etc.

Some examples of interactions constrained in the indirect manner are shown in Fig. 18. Fig. 18a depicts the modified interaction described in Section 2.3. Because the extent of mainstream flow taken into the channel between the plates is large, the degree of constraint imposed on the interaction is small. About the only noticeable feature is an indication of further shock waves downstream of the main system, suggesting a more extensive persistence of supersonic flow than in the basic case. A more considerable effect from the pressure field of the control surface flap – not properly seen in the photograph – is discussed in Sections 4.2 and 5.

In Fig. 18b the control surface has been brought down close to the vortex sheet and angled slightly. Flow modifications are somewhat more extensive than in Fig. 18a. Viscous-layer growth is greater, as is also the extent of supersonic flow in the intermediate layer. The intermediate layer reveals a succession of normal shocks, associated perhaps with irregularities in the 'edge' of the viscous layer.

In a third example (Fig. 18c) the flow channel has been restricted so as to push the shock out ahead of the control surface in a manner illustrating flow spillage. In this case the separation effect is magnified considerably and the turbulent mixing region appears to be spreading rapidly across the full width of the channel.

The second way in which an interaction may be modified is by direct alteration to the solid surface, e.g. by terminating it or inclining it to the mainstream direction. A case in point is that of the transonic flow over an aerofoil, depicted in Fig. 1a. A common situtation is that owing to the wing surface being

inclined away from the stream direction and terminated at the trailing edge, the flow does not reattach after separation, closure of the bubble occurring instead some distance behind the trailing edge. This type of contraint is important also in the case of intakes and ducts, where curvature of the surface close behind a position of shock interaction may have a considerable effect on the magnitude of total pressure loss sustained.

Modified interactions, then, have considerable practical significance. Some basic experimental investigations introducing the effects of surface curvature or inclination and of mainstream flow constraints after the manner described would be valuable.

4.2. *The Modified Interaction.*

Results for the particular modified interaction introduced in Section 2.3 are presented in Figs. 19 and 20. The curve of surface pressure distribution in Fig. 19, when compared with that for the basic interaction (Fig. 7) shows that the rear expansion affects the flow before the pressure recovery after separation has been completed. This is the chief difference between the modified and basic conditions. Up to a distance of 20 initial boundary-layer thicknesses, results are substantially the same for both. Examination of profiles (3) and (4) in Fig. 20 leads to the suggestion that the extent of the bubble has been reduced slightly by the constraining effect of the control surface, but the change is small.

The first effect of the rear expansion field is to speed up profile rehabilitation following reattachment. Thus profile (11) (Fig. 20) at $x/\delta_u = 34$, is closer to the initial profile than is profile (12) of the basic interaction (Fig. 11), at $x/\delta_u = 52$.

The effect goes further, however, in that profiles (12) to (14) of the modified interaction are appreciably fuller than the initial profile. These features of the rear expansion flow are of interest in the general consideration of profile similarities which follows.

5. *Profile Similarities.*

5.1. *The Coles Wake Hypothesis.*

An important advance in the study of the turbulent boundary layer has been made by Donald Coles in a paper[7] in the Journal of Fluid Mechanics (1956). Following an extensive study of velocity profiles obtained, by other experimenters, in various two-dimensional incompressible turbulent boundary-layer flows, Coles has advanced the hypothesis that the general profile can be represented by a linear combination of two universal functions. One is the well-known law of the wall. The other, called the law of the wake, links the development of the turbulent boundary layer with that of an equivalent wake profile which, it is suggested, represents the large-eddy structure. Introduction of the law of the wake is Coles' particular contribution. The existence – and persistence – of profile similarity in these terms is convincingly demonstrated in the flows analysed by him and there is little doubt that the hypothesis makes a valuable approach to the expression of physical reality.

In a flow passing through separation and reattachment it is to be expected that the law of the wall will, temporarily at least, lose much of its influence on the profile and any wake structure will become dominant. It is therefore interesting and important to examine the results of the present investigation in the light of the Coles hypothesis.

Coles writes the general profile in the form

$$\frac{u}{u_\tau} = \frac{1}{K}\log\frac{y\,u_\tau}{\nu} + C + \frac{\pi}{K}\,w\left(\frac{y}{\delta}\right). \tag{1}$$

In this, u_τ is the friction velocity, defined by

$$\rho\,u_\tau^2 = \tau_w, \tag{2}$$

τ_w being the value of shear stress at the surface: $1/K$ and C are the constants in the law of the wall, which is represented by the first two terms on the right hand side: π is a form parameter, whose value determines the strength of the wake component. In terms of more usual boundary-layer parameters, π is determined by the relationship:

$$\frac{\pi+1}{K} = \frac{\delta^*}{\delta}\frac{u_1}{u_\tau}. \tag{3}$$

$w(y/\delta)$ is, according to the hypothesis, a universal function common to all two-dimensional, incompressible turbulent-boundary layer flows. This function, as determined and tabulated by Coles, is plotted in Fig. 21.

Since we are here concerned primarily with the wake component and only incidentally with the wall component of the layer, it is convenient to express the velocity ratio in terms of u_1, the value at the outer edge of the layer, rather than u_τ. We have from (1)

$$\frac{u}{u_1} = \frac{u_\tau}{K u_1}\log\frac{y u_\tau}{\nu} + C\frac{u_\tau}{u_1} + \frac{\pi u_\tau}{K u_1} w. \tag{4}$$

On the edge of the layer

$$1 = \frac{u_\tau}{K u_1}\log\frac{\delta u_\tau}{\nu} + C\frac{u_\tau}{u_1} + 2\frac{\pi u_\tau}{K u_1}, \tag{5}$$

(the function w having been normalised in such a way that its value at $y = \delta$ is 2).

Combining (4) and (5) gives

$$1 - \frac{u}{u_1} = \frac{u_\tau}{K u_1}\log\frac{\delta}{y} + \frac{\pi u_\tau}{K u_1}(2-w);$$

or if, for brevity, we write

$$\frac{\pi u_\tau}{K u_1} \equiv P, \tag{6}$$

$$1 - \frac{u}{u_1} = \frac{u_\tau}{K u_1}\log\frac{\delta}{y} + P(2-w). \tag{7}$$

The construction of a general turbulent profile according to this expression is illustrated in Fig. 22.*

5.2. *Extraction of wall friction term.*

In order to analyse the measured profiles it is necessary first to assume an overall validity of the law of the wall. The form:

$$\frac{u}{u_\tau} = 5{\cdot}75\log_{10}\frac{y u_\tau}{\nu_w} + 5{\cdot}10 \tag{8}$$

has been assumed to apply throughout the flow, whatever the pressure gradients, ν_w being the value of kinematic viscosity corresponding to an estimated wall temperature.

---

*The logarithmic law of the wall is, of course, invalid very close to the surface, where the velocity tends to zero. We are not however concerned with this particular divergence.

A logarithmic plot of any profile within the regions of attached flow (i.e. before separation or after reattachment) reveals a linear portion corresponding to the logarithmic law. Obtaining by trial and error the best fit of this portion to equation (8), a value of u_τ is deduced.

Fig. 23 illustrates the fit of the initial boundary-layer profile to the law of the wall. Deduced values relating to conditions at the surface are given on the diagram. It is noted in passing that the value of local shear stress, $\tau_w/q_1 = 0{\cdot}0024$, is four-fifths of the value of average skin-friction coefficient ($C_F = 0{\cdot}0030$) as obtained from a calculation of momentum thickness made directly from the measured profile.

Logarithmic plots of several profiles from the modified interaction are shown in Fig. 24. Corresponding values of friction velocity ratio are plotted in Fig. 28. It is seen that the local friction intensity falls to zero at separation, rises steadily after reattachment, and in the case of the modified interaction, overshoots the initial value owing to the effect of flow acceleration.

In Fig. 24 the digressions from the linear law are essentially similar throughout the region labelled 'after reattachment' but those of the profiles before separation and in the accelerating flow are different in character.

5.3. *Wake Components.*

Wake components of the profiles can now be examined by removing the term

$$\frac{u_\tau}{K u_1} \log \frac{\delta}{y}$$

from the complete measured profile. In the case of profiles close to separation and reattachment – including those in the bubble region – it is sufficient to ignore the friction term except for one or two points very near the surface.

It is found that for the undisturbed layer and for all profiles from reattachment onwards, except for those in the accelerating flow of the modified interaction, the wake components conform closely to the form given by Coles which, from equation (7), is:

$$\frac{u}{u_1} = 1 - P(2 - w), \tag{9}$$

where the value of P is determined by the wall condition:

$$P = \frac{1}{2}\left[1 - \left(\frac{u}{u_1}\right)_{y=0}\right]. \tag{10}$$

Examples of the conforming profiles are given in Fig. 25.

The effect of compressibility on the comparisons has been estimated in one case, that of the near-reattachment profile of Fig. 25. The Coles wake-profile was modified by means of a Howarth transformation of y-ordinates:

$$y' = \int_0^y \frac{\rho}{\rho_1} dy\,; \qquad \delta' = \int_0^\delta \frac{\rho}{\rho_1} dy\,. \tag{11}$$

The modified profile differs from the original in a direction tending to improve agreement with the experimental results. The change is small, however, and since in the particular case chosen the range of density variation was greater than for most of the profiles, it seems permissible for present purposes to neglect the compressibility effect.

The results confirm, therefore, that over a large part of the flow, profile similarity exists in the form suggested. In particular the reattachment profile is itself of the Coles wake form, with consequently a value of δ^*/θ in agreement with his prediction as was mentioned in Section 3.3.

Turning to the remaining regions of the flow, it is found that in the initial pressure rise and for some time after separation, profile similarity is not maintained. The same conclusion applies to the region of rapid pressure fall in the modified interaction. Examples of wake components from these regions are shown in Fig. 26. Clearly there is substantial distortion as compared with the Coles wake profile scaled to the same value of u/u_1 at $y = 0$. Undoubtedly this represents an effect of large pressure gradients, such as that imposed by the shock wave, in disturbing the equilibrium of inertia mixing forces within the layer.

Thus the Coles wake hypothesis is to be qualified to the extent that where large pressure gradients exist in the flow, such as those produced by shock waves, the combination of wall and wake laws does not adequately describe the boundary-layer development at all stages.

It is interesting that the strong favourable pressure gradient of the modified interaction should produce distortion opposite in sign yet similar in character to that produced by the shock wave. Fig. 27 shows that, in fact, all the distortions measured can, to a first approximation, be represented by a single empirical function of y/δ, coupled with a scaling factor which, as with the wake parameter P, is a function of x only. That is, the distortion velocity can be written as:

$$\frac{\Delta u}{u_1} = Q(x)\, t\left(\frac{y}{\delta}\right) \tag{12}$$

and the complete profile takes the form:

$$1-\frac{u}{u_1} = \frac{u_\tau}{K u_1}\log\frac{\delta}{y} + P(x)\left[2-w\left(\frac{y}{\delta}\right)\right] - Q(x)\, t\left(\frac{y}{\delta}\right) \tag{13}$$

The turbulent-layer development throughout the whole interaction can be represented in this form. Values of the profile parameters u_τ/u_1, P and Q for the basic and modified interactions are plotted in Fig. 28. Comment on the variations of friction velocity has already been made. The wake parameter P has initially a low value (0·04) but rises to the order of 0·5, which by definition is the precise value for both separation and reattachment. The variation of P is generally of inverse character to that of u_τ/u_1; in fact as a rough empiricism it may be suggested that the following holds:

$$a\,P + b\frac{u_\tau}{u_1} = 1 \tag{14}$$

with values, in the present case:

$$a = 2; \qquad b = 24$$

The distortion parameter increases rapidly from zero during the shock phase and is a maximum at separation. The value decreases during the displacement phase and is zero again throughout the greater part of the normal rehabilitation. In the modified interaction 'negative' distortion occurs during the acceleration phase and reaches a level of magnitude about half that produced by the shock wave.

6. *Conclusions.*

(1) The nature of the interaction between a turbulent boundary layer and a strong normal shock in two-dimensional flow has been examined. Emphasis has been placed on the downstream flow development. Separation and reattachment are demonstrated and the character of the eddy-flow bubble in the separated region is revealed.

(2) Shock bifurcation is an essential feature of the flow. Because of this, the total flow field breaks down into three régimes, in which distinct sets of boundary conditions require to be satisfied simultaneously. The three régimes are:

(i) the mainstream flow through the normal shock;

(ii) an intermediate layer of flow through the bifurcated shock systems;

(iii) the viscous layer.

(3) Conditions in each of the régimes are described. The existence of mixed supersonic and subsonic flow in the intermediate layer is revealed. The overall flow process within the viscous layer is seen to consist of three phases:

(a) the shock phase;

(b) the displacement phase;

(c) the rehabilitation phase.

Examination of pressure distributions, velocity profiles and the standard boundary-layer parameters shows the particular characteristics of each development phase.

(4) In the two particular flows examined in detail, the boundary layer was formed on a flat plate. The mainstream flow was in one case virtually constraint-free and in the other case constrained in a rather special way. The ways in which boundary conditions generally affect the flow development are discussed and suggestions for further experiment, employing other forms of constraint, are made.

(5) Viscous-layer velocity profiles throughout the whole extent of interaction, including the region of separated flow, are examined in relation to the Coles hypothesis of profile similarities for the turbulent layer. This examination shows that, broadly speaking, profile similarity, in the sense defined by Coles, exists in the initial layer, is disturbed during the shock phase, restored during the displacement phase, and exists again throughout the long phase of rehabilitation.

(6) The profile distortion which occurs during the shock phase is caused by the sudden pressure rise in the streamwise direction. The distortion has a characteristic form and the Coles hypothesis may be extended, empirically, to include a 'distortion' term similar in form to his 'wake' term. In this extended form, which is now a linear combination of the law of the wall, the law of the wake and a 'law of distortion', the similarity hypotheses can be applied to the complete interaction flow. The extended hypothesis may be expected to apply generally to the turbulent boundary layer in a two-dimensional flow with arbitrary pressure gradients.

Acknowledgement.

Acknowledgement is made to all members of the Aero Staff of GALCIT for help given unstintingly. Thanks are due especially to the late Professor C. B. Millikan for ready cooperation in making arrangements and providing facilities; to Professor H. W. Liepmann, with whom to work was a privilege and from whose interest stemmed much helpful advice and stimulating discussion; and to Dr. Donald Coles with whom points of common interest were repeatedly and advantageously talked over. The assistence of Dr. W. W. Willmarth, J.P. Gorecki and M. C. Lock with the experiment is also gratefully acknowledged. The Report was first presented to the AGARD specialists meeting on 'Boundary-layer Research', held in London in April 1960.

LIST OF REFERENCES

No.	*Author(s)*	*Title, etc.*
1	H. H. Pearcey	A method for the prediction of the onset of buffeting and other separation effects from wind-tunnel tests on rigid models. ARC.20, 631. December, 1958.
2	J. Seddon and L. Haverty ..	Experiments at Mach numbers from 0·5 to 1·8 on side intakes of normal-shock type without boundary layer control (Part I). R.A.E. Tech. Note Aero. 2329. ARC.17398. October, 1954.
3	J. Seddon	Boundary-layer interaction effects in intakes with particular reference to those designed for dual subsonic and supersonic performance. R.A.E. Tech. Report No. 66 099 – ARC.28368. March 1966.
4	C. F. Griggs and E. L. Goldsmith	Shock oscillation ahead of centre-body intakes at supersonic speeds. R.A.E. Report Aero. 2477. ARC.15634. September, 1952.
5	G. E. Gadd	Interactions between wholly laminar or wholly turbulent boundary layers and shock waves strong enough to cause separation. *J. Aero. Sci.*, Vol. 20, No. 11, pp. 729–739. 1953.
6	S. M. Bogdonoff and C. E. Kepler	Separation of a supersonic turbulent boundary layer. *J. Aero. Sci.*, Vol. 22, No. 6, pp. 414–424 & 430. 1955.
7	Donald Coles	The law of the wake in the turbulent boundary layer. Journ. Fluid Mech. Vol. I, pp. 191–226. 1956.

NOTATION

x distance downstream of start of interaction

y distance above surface of plate

V velocity in mainstream

u local velocity

M Mach number

ρ density

q $\frac{1}{2}\rho V^2$

p static pressure

p_0 total pressure

δ viscous-layer thickness (defined to 0·999 velocity ratio)

δ^* displacement thickness, defined by:

$$\delta^* = \int_0^\delta \left(1 - \frac{\rho u}{\rho_1 u_1}\right) dy$$

θ momentum thickness defined by:

$$\theta = \int_0^\delta \frac{\rho u}{\rho_1 u_1} \left(1 - \frac{u}{u_1}\right) dy$$

H form parameter, δ^*/θ

R Reynolds number

C_F mean skin-friction coefficient

y' transformed ordinate, $y' = \int_0^y \frac{\rho}{\rho_1} dy$

δ' transformed thickness, $\delta' = \int_0^\delta \frac{\rho}{\rho_1} dy$

τ shear stress

u_τ friction velocity, defined by $\rho_w u_\tau^2 = \tau_w$

ν kinematic viscosity

K,C constants in Law of the Wall

w Coles wake function

π	Coles wake parameter
P	wake parameter defined by $P = \dfrac{\pi u_1}{K u_1}$
t	distortion function
Q	distortion parameter

Suffixes:

∞	free stream conditions
1	local conditions at edge of viscous layer
w	wall conditions

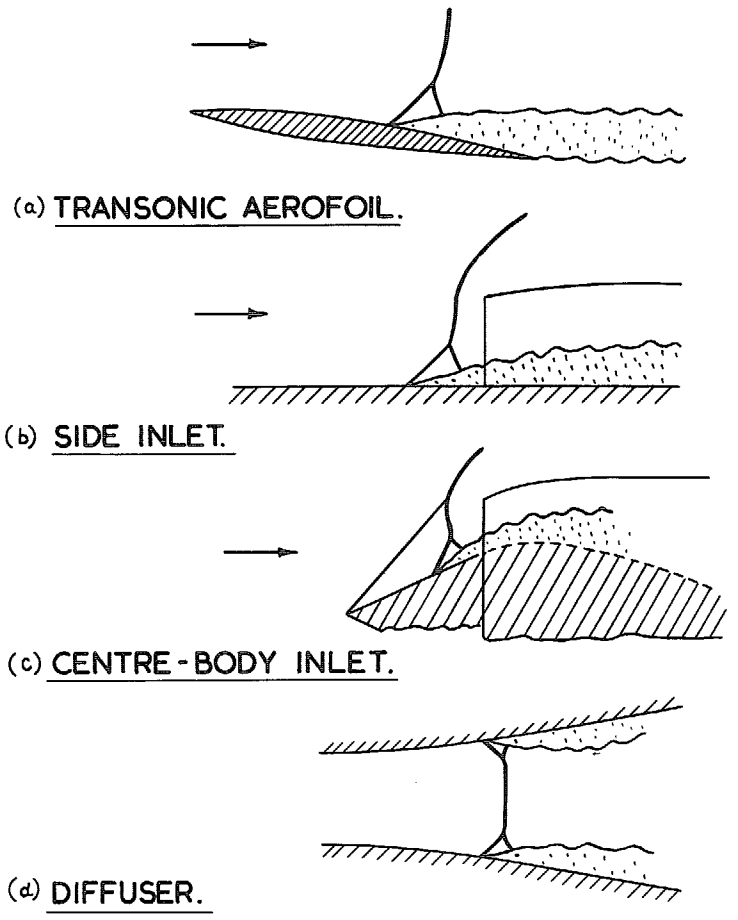

FIG. 1. Examples of interaction of turbulent boundary layer and normal shock wave.

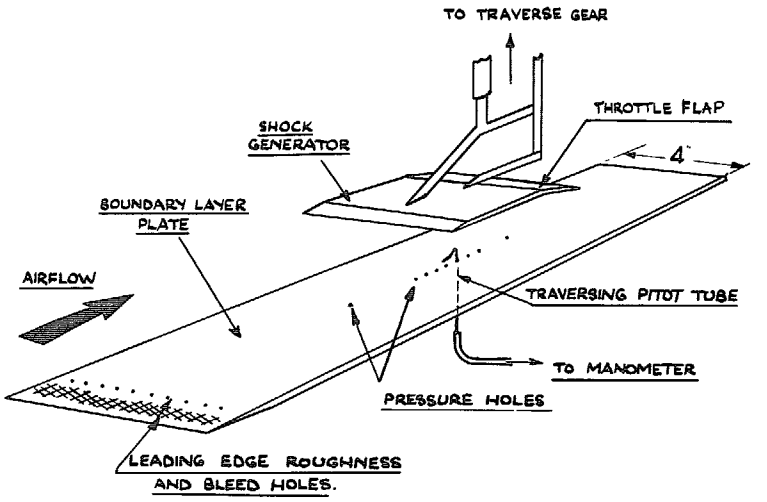

FIG. 2. Experimental arrangement (GALCIT 10 in. × 4 in. tunnel).

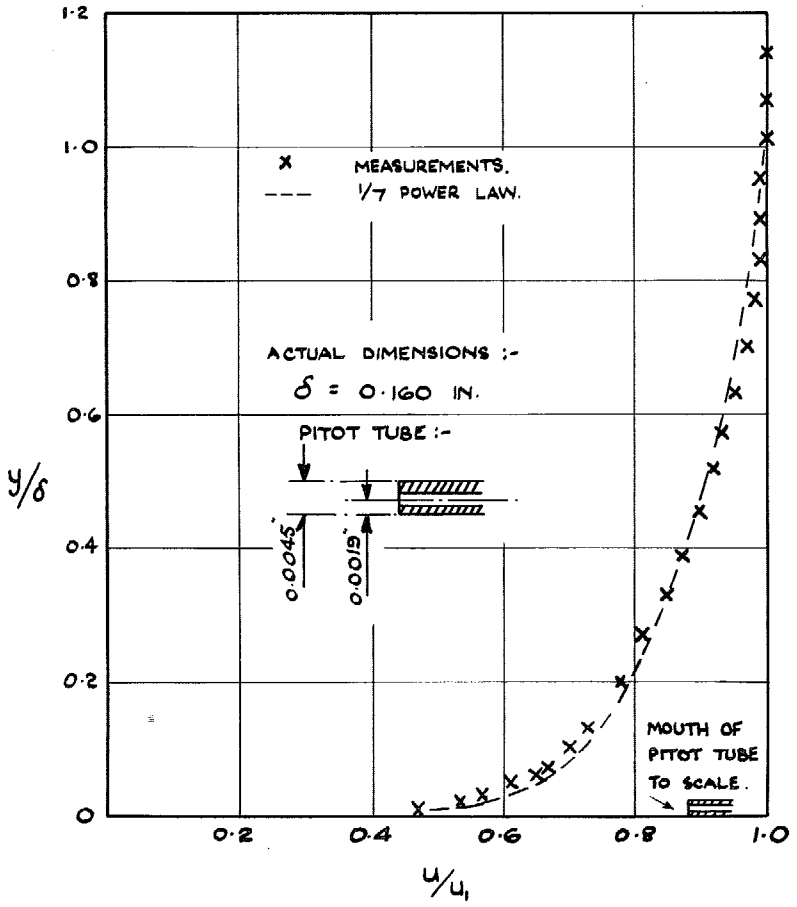

FIG. 3. Profile of undisturbed boundary Layer ($M = 1{\cdot}47$).

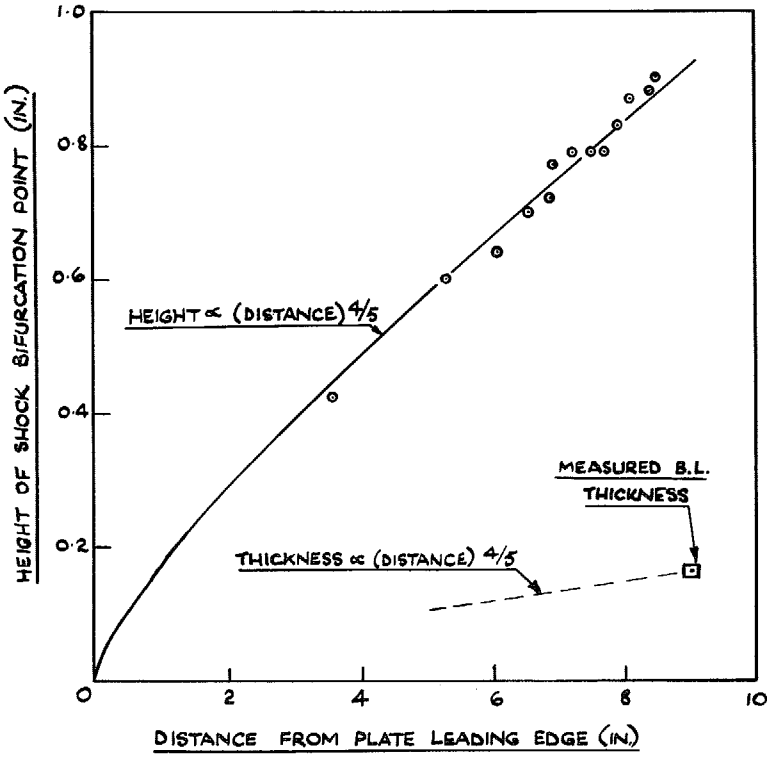

FIG. 4. Correction for variation of initial boundary-layer thickness.

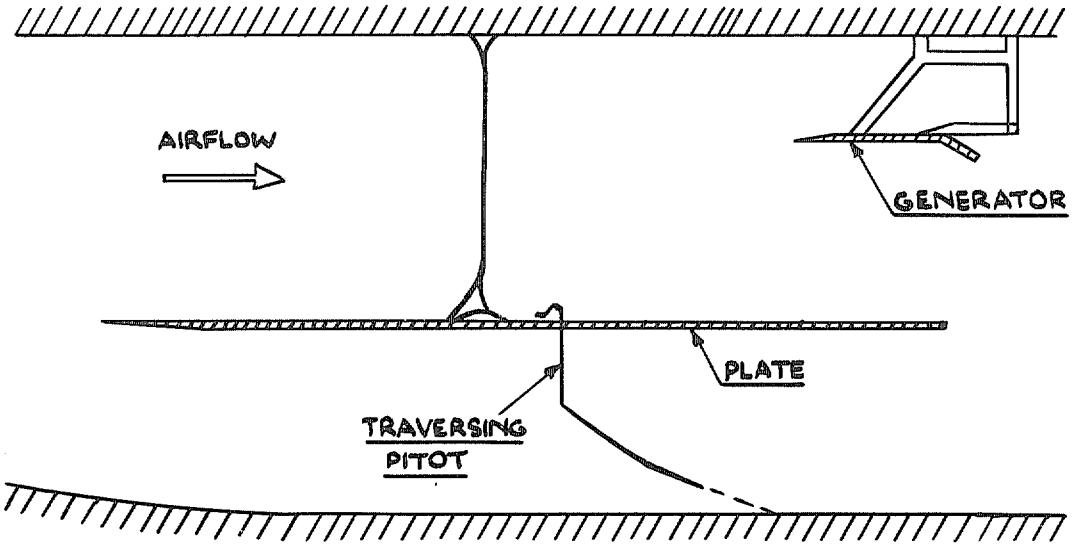

FIG. 5a. Basic interaction.

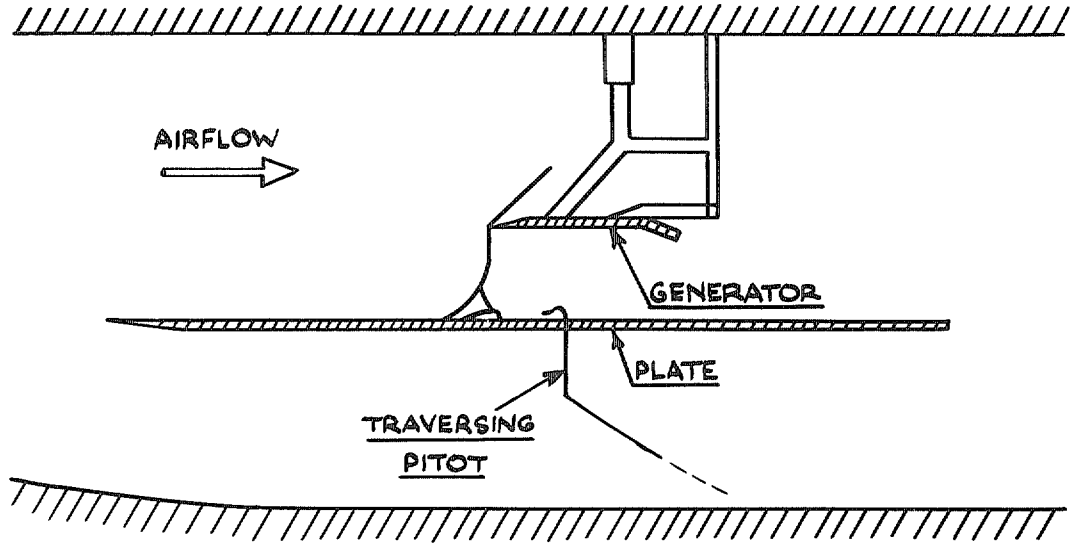

FIG. 5b. Modified interaction.

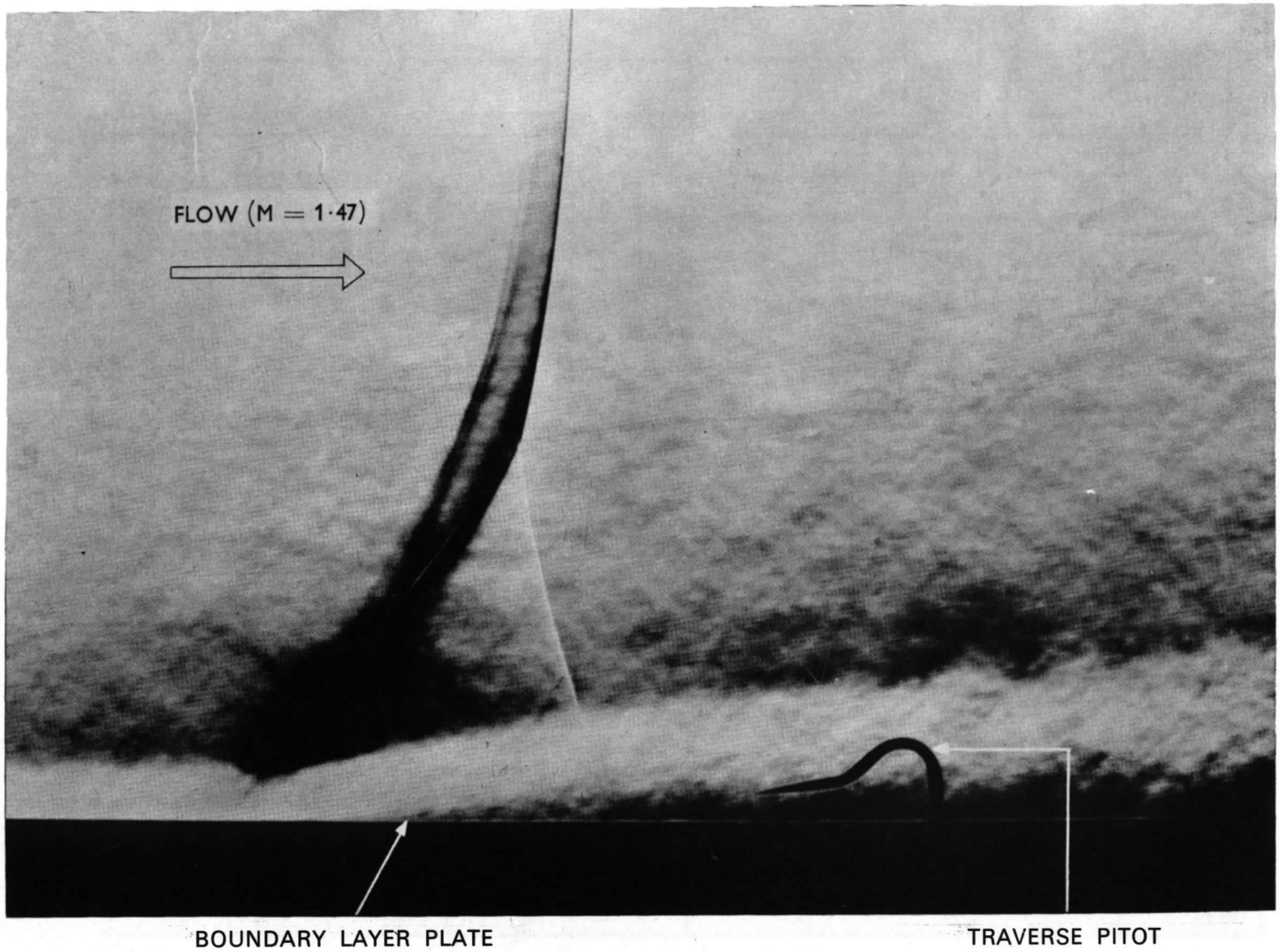

FIG. 6. Basic interaction.

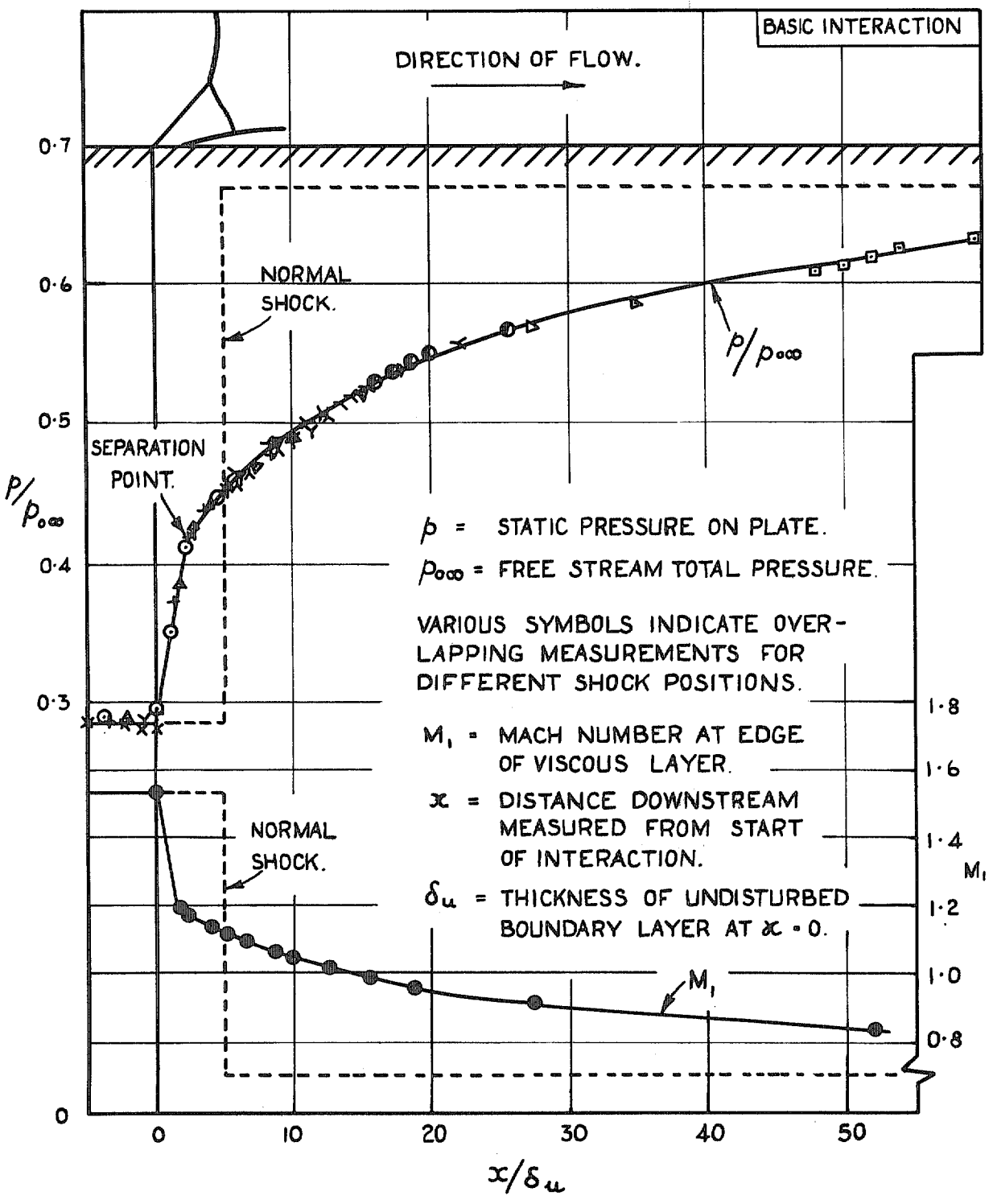

FIG. 7. Surface pressure distribution and Mach No. outside viscous layer.

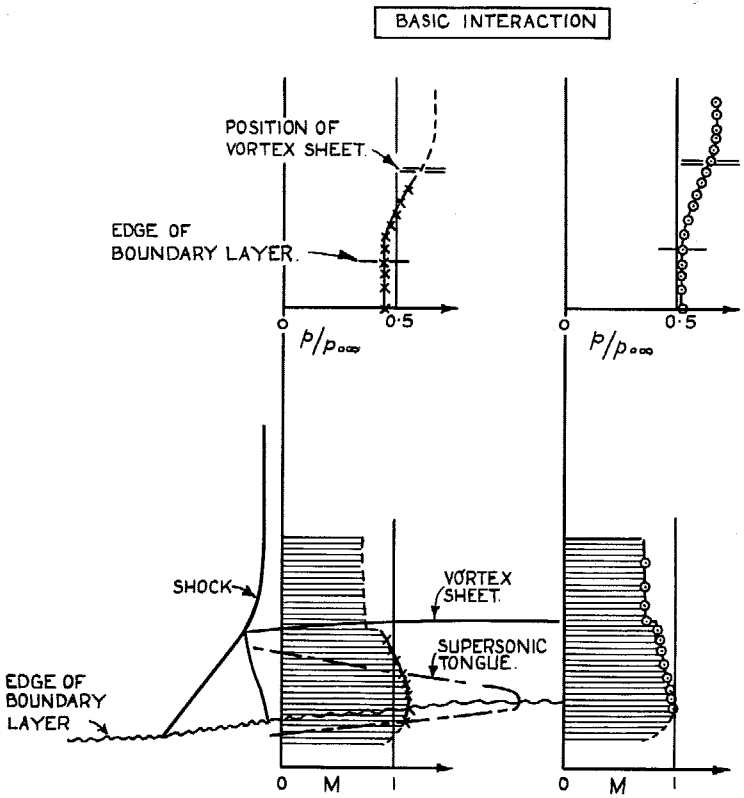

FIG. 8. Static-pressure traverses normal to plate leading to definition of supersonic tongue.

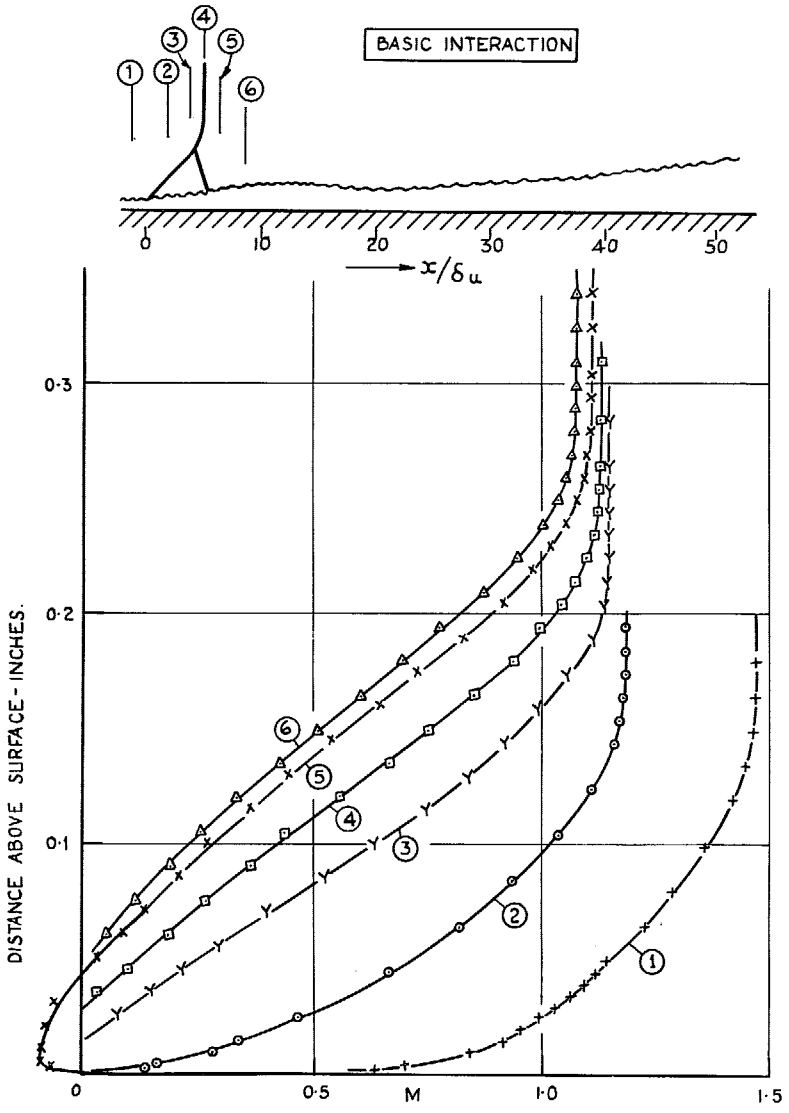

FIG. 9. Boundary-layer traverses: Mach profiles 1 to 6.

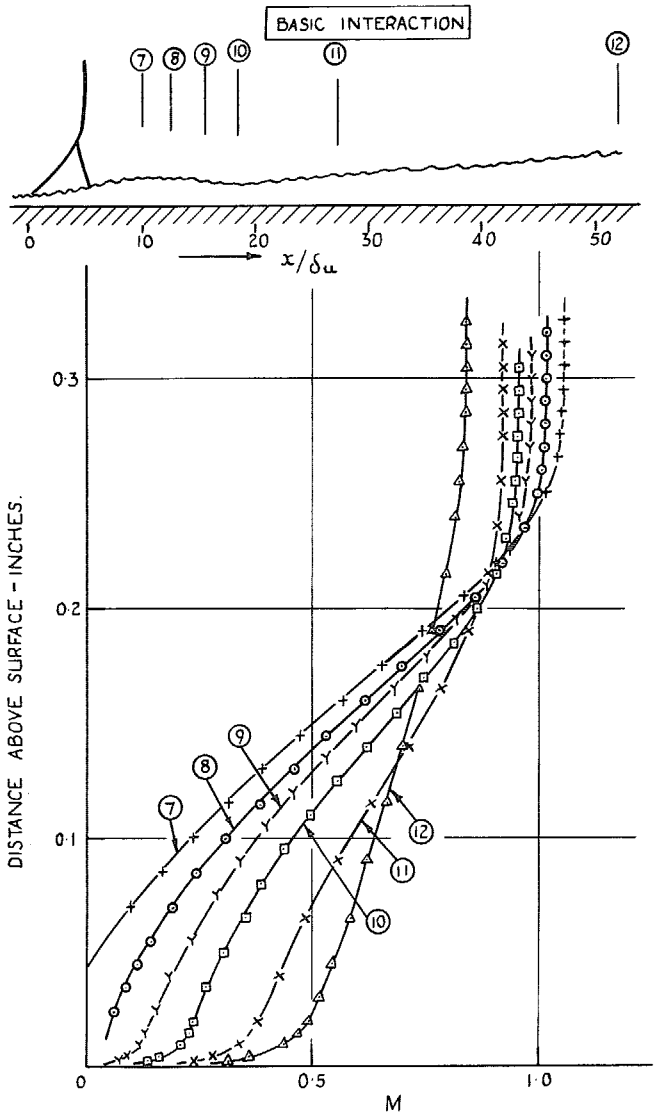

FIG. 10. Boundary-layer traverses: Mach profiles 7 to 12.

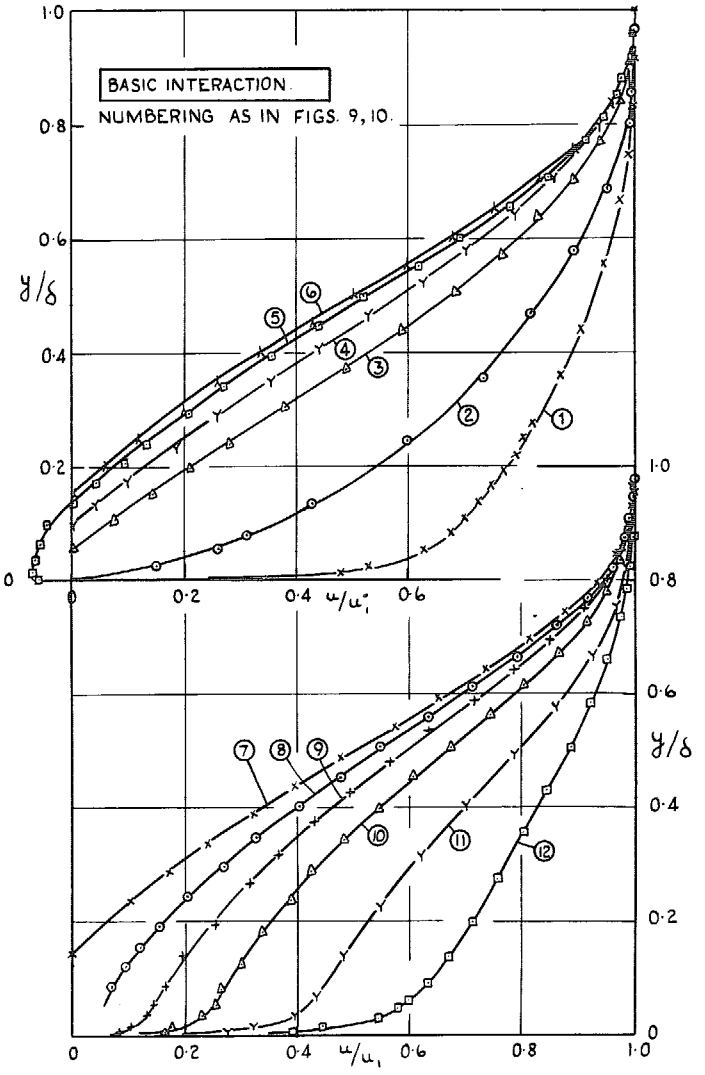

FIG. 11. Non-dimensional velocity profiles.

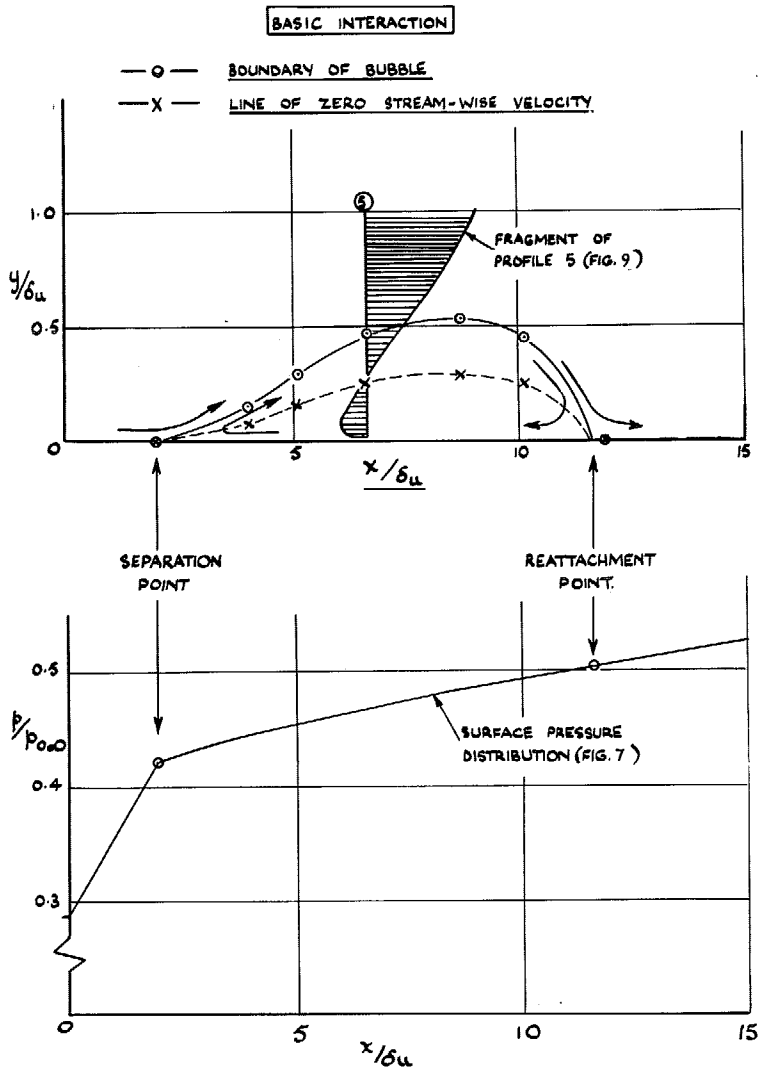

FIG. 12. Details of separation bubble.

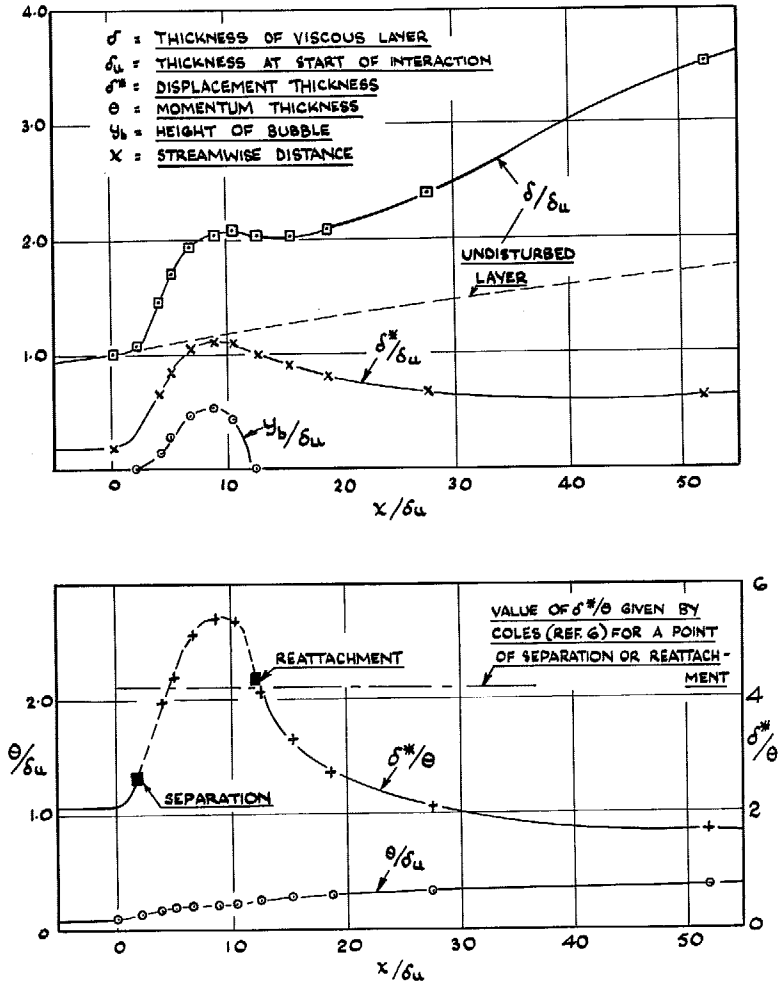

FIG. 13. Viscous-layer Parameters for basic interaction.

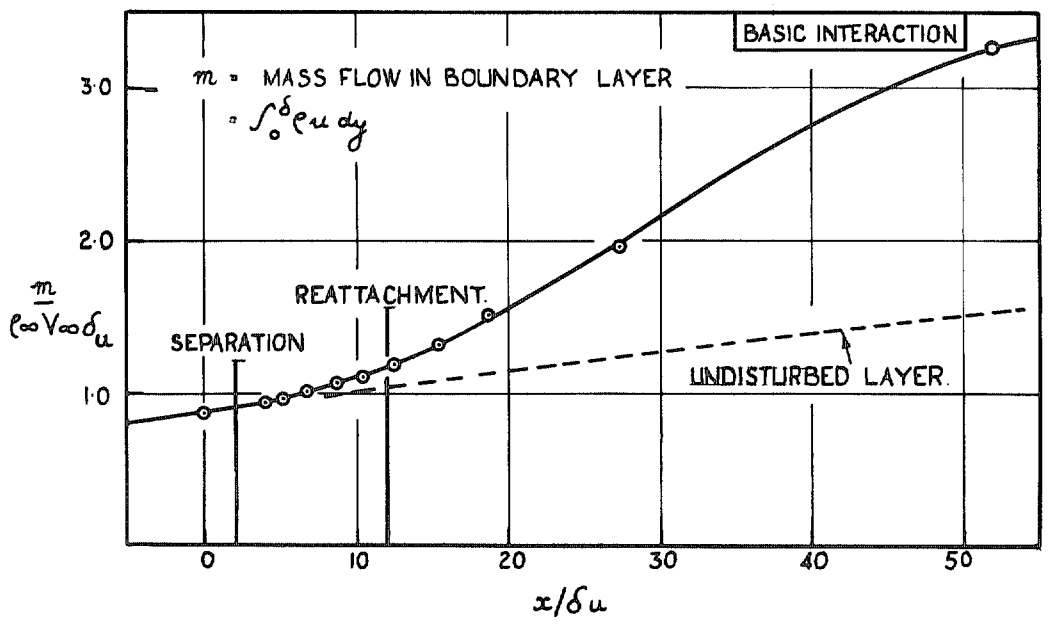

FIG. 14. Mass flow.

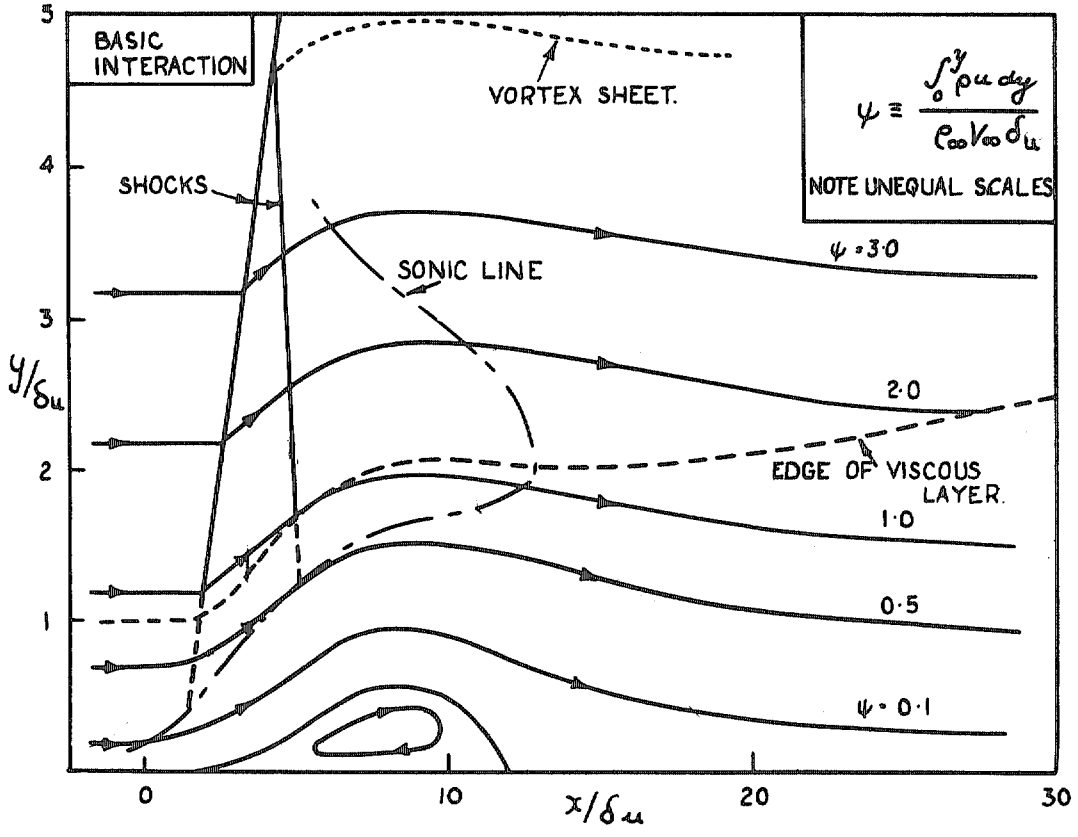

FIG. 15. Calculated streamlines.

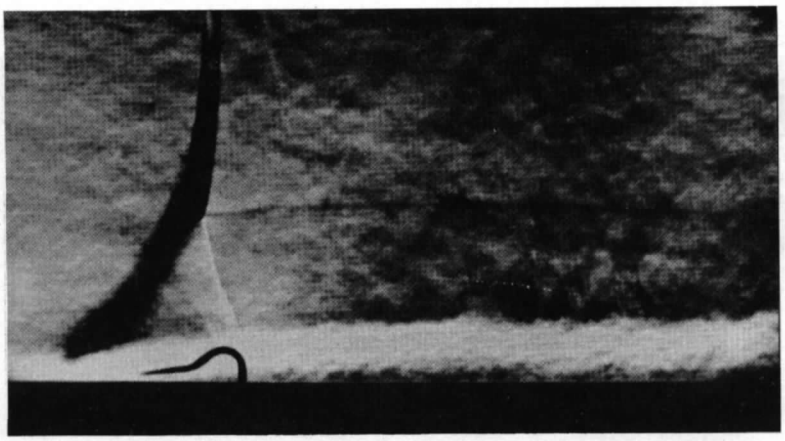

(a)

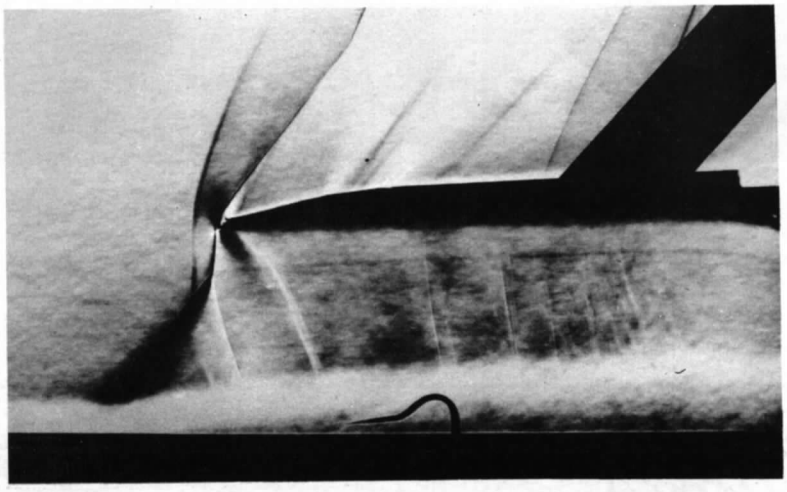

(b)

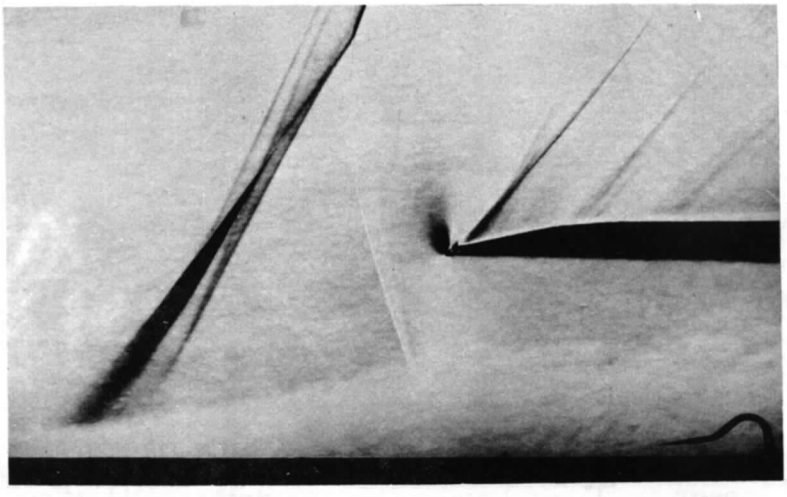

(c)

FIG. 18. Interactions with external constraint.

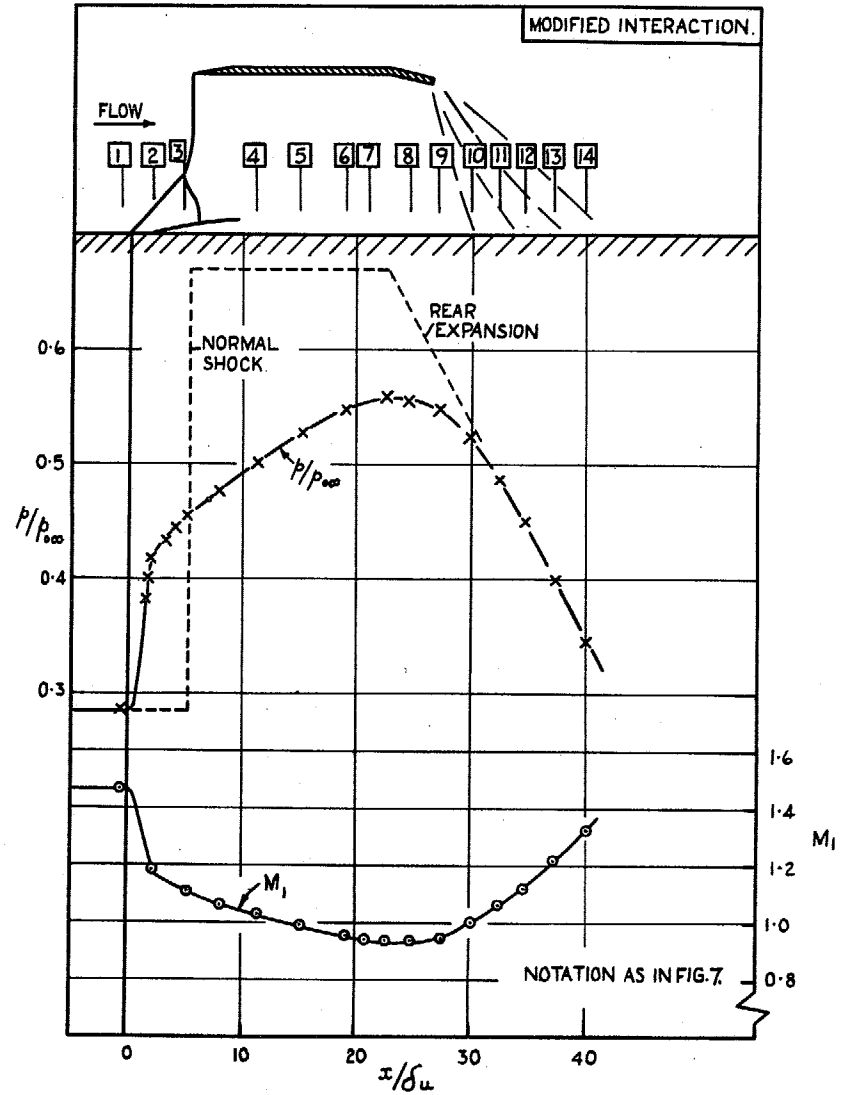

FIG. 19. Surface pressure distribution and Mach No. outside viscous layer. (Modified interaction).

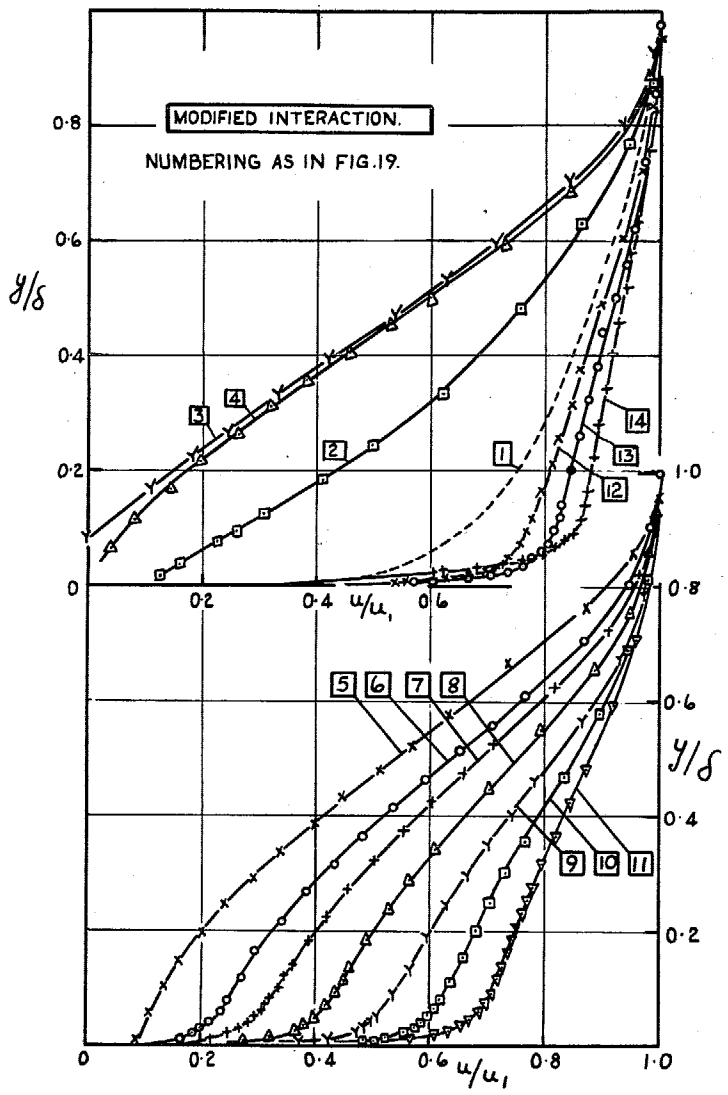

FIG. 20. Non-dimensional velocity profiles.

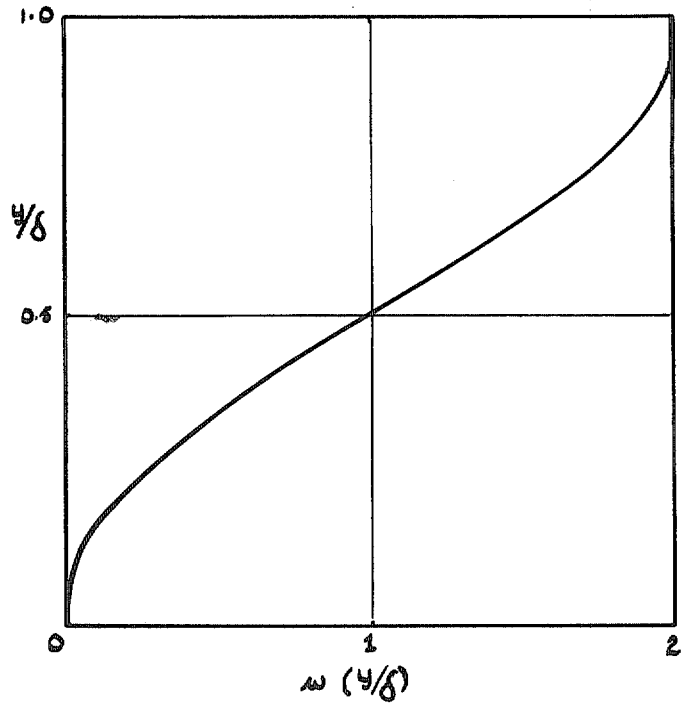

FIG. 21. Coles' wake function.

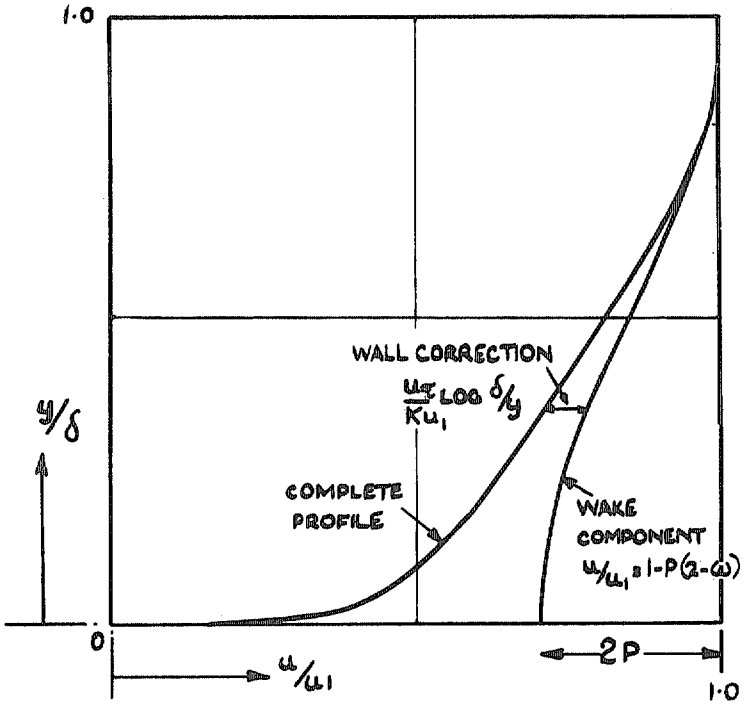

FIG. 22. General profile according to eqn. 7.

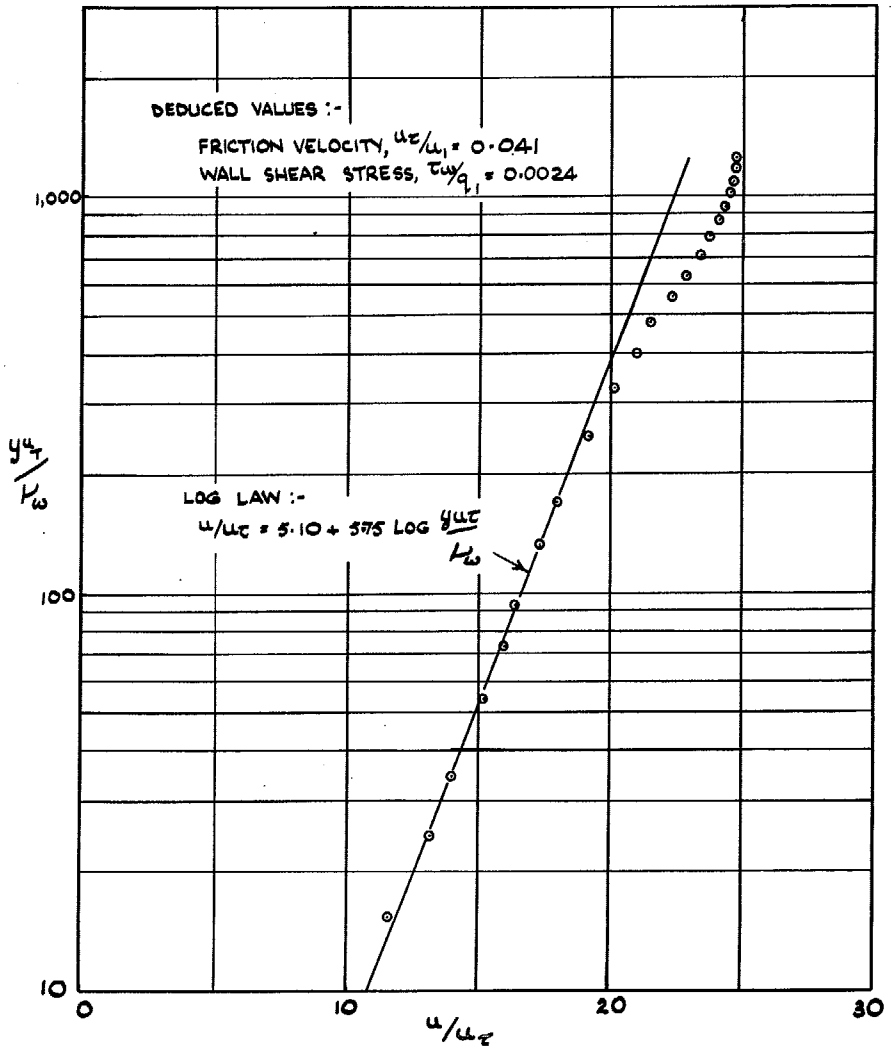

FIG. 23. Curve fitting for initial boundary-layer profile.

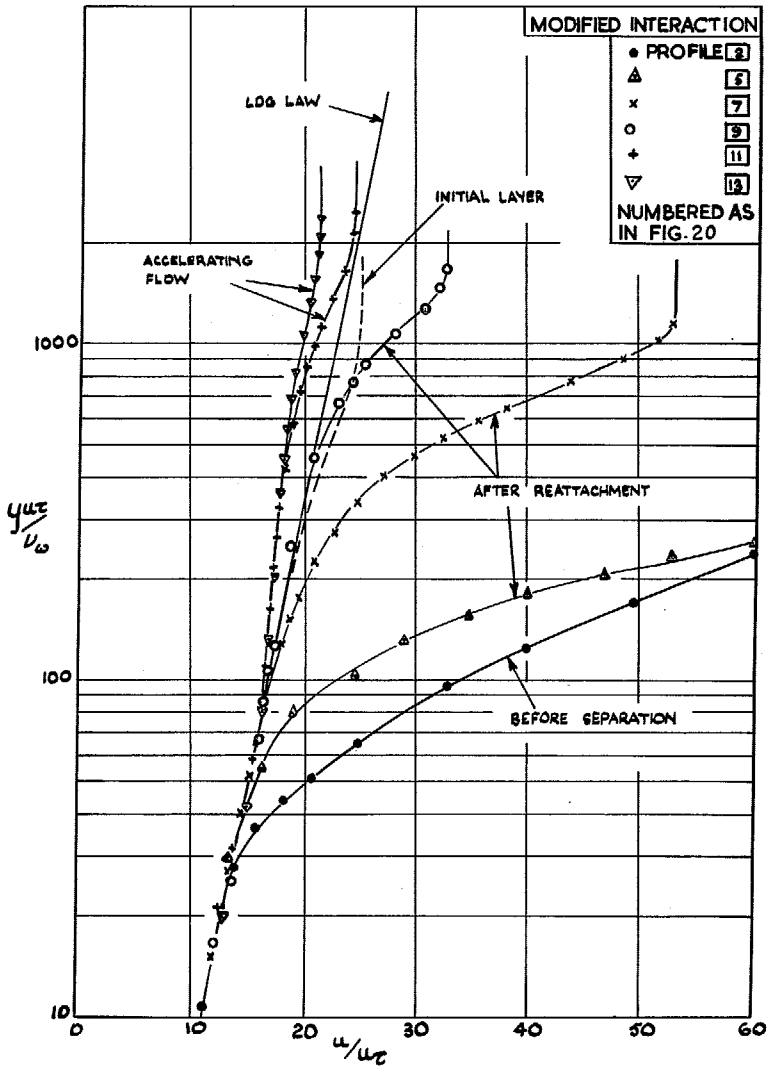

FIG. 24. Curve fitting for interaction layers.

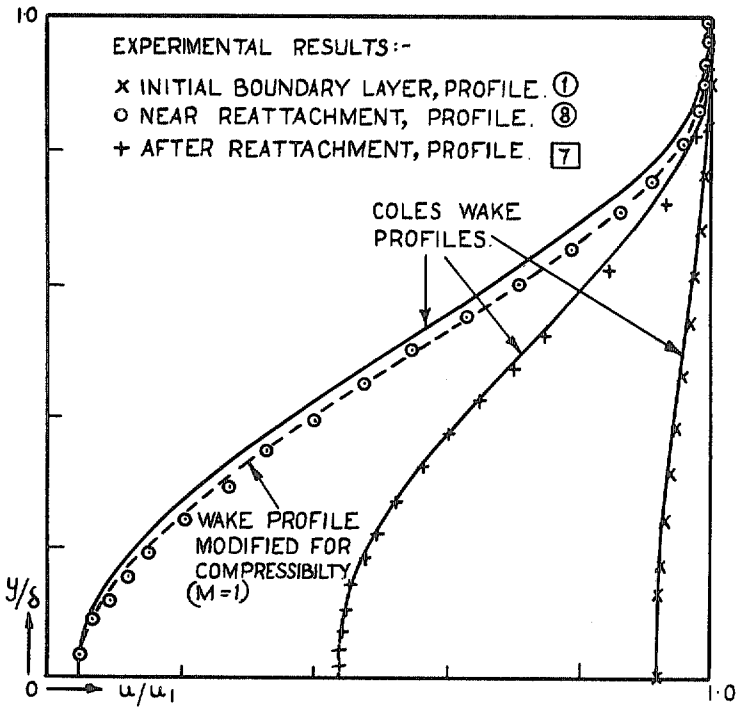

FIG. 25. Conforming wakes.

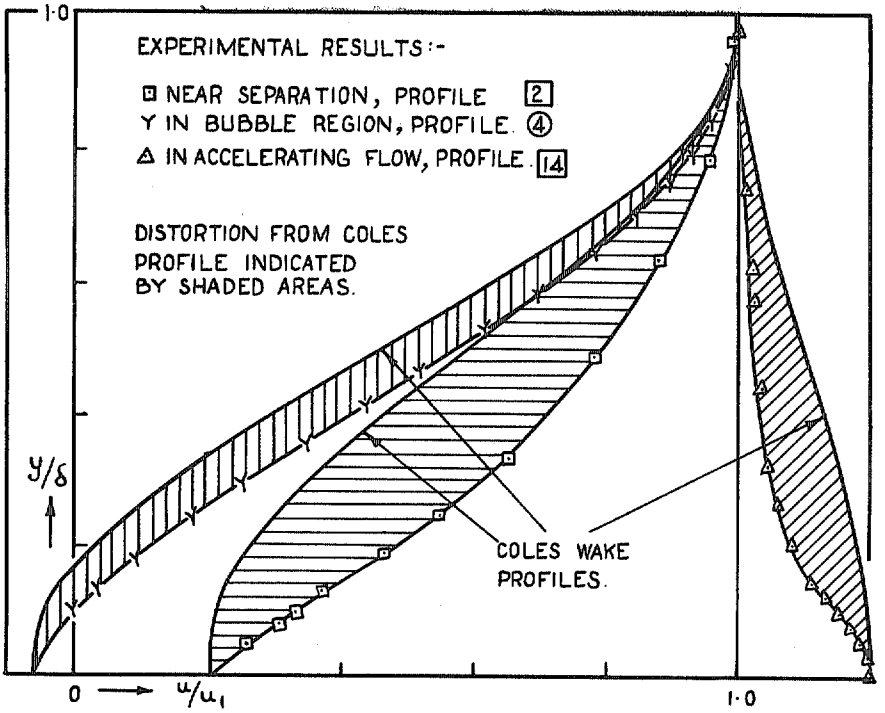

FIG. 26. Distorted wakes.

Printed in Wales for Her Majesty's Stationery Office by Allens Printers (Wales) Limited.
D.129527 K5

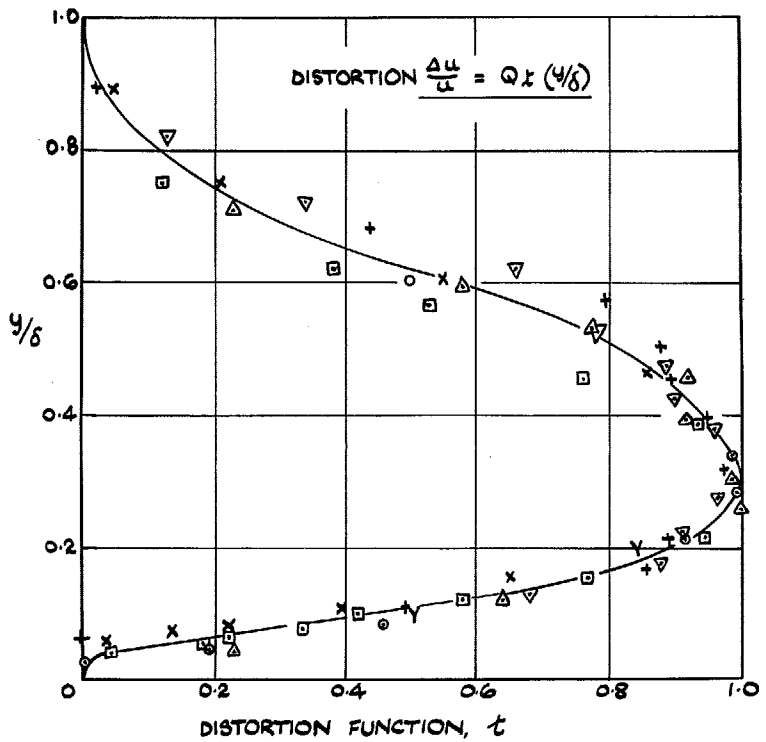

FIG. 27. Approximate correlation of profile distortions.

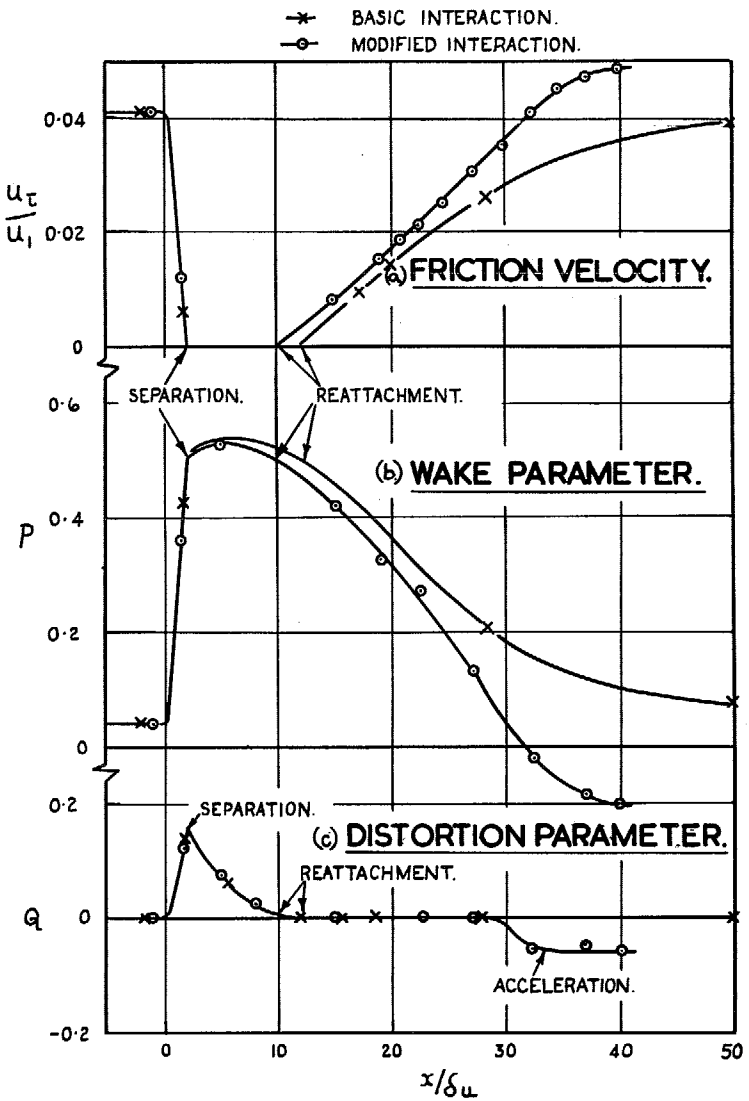

FIG. 28. Profile parameters for basic and modified interactions.

Published by
HER MAJESTY'S STATIONERY OFFICE

To be purchased from
49 High Holborn, London W.C.1
423 Oxford Street, London W.1
13A Castle Street, Edinburgh 2
109 St. Mary Street, Cardiff
Brazennose Street, Manchester 2
50 Fairfax Street, Bristol 1
35 Smallbrook, Ringway, Birmingham 5
7–11 Linenhall Street, Belfast 2
or through any bookseller

S.O. Code No. 23 350